Inorg. Chem. **2008**, *47*, 980–989

Synthesis, Characterization, and DFT/TD-DFT Calculations of Highly Phosphorescent Blue Light-Emitting Anionic Iridium Complexes

Davide Di Censo,[†] Simona Fantacci,*[,‡] Filippo De Angelis,[‡] Cedric Klein,[†] Nick Evans,[†] K. Kalyanasundaram,[†] Henk J. Bolink,[§] Michael Grätzel,[†] and Mohammad K. Nazeeruddin*[,†]

Laboratory for Photonics and Interfaces, Station 6, Institute of Chemical Sciences and Engineering, School of basic Sciences, Swiss Federal Institute of Technology, CH - 1015 Lausanne, Switzerland, Istituto CNR di Scienze e Tecnologie Molecolari (ISTM-CNR), c/o Dipartimento di Chimica, Università di Perugia, I-06123, Perugia, Italy, and Institute of Molecular Science, University of Valencia, P.O. Box 22085 ES-46071 Valencia, Spain

Received September 14, 2007

Highly phosphorescent blue-light-emitting anionic iridium complexes $(C_4H_9)_4N[Ir(2\text{-phenylpyridine})_2(CN)_2]$ (**1**), $(C_4H_9)_4N[Ir(2\text{-phenyl-4-dimethylaminopyridine})_2(CN)_2]$ (**2**), $(C_4H_9)_4N[Ir(2\text{-(2,4-difluorophenyl)-pyridine})_2(CN)_2]$ (**3**), $(C_4H_9)_4N[Ir\text{-}(2\text{-(2,4-difluorophenyl)-4-dimethylaminopyridine})_2(CN)_2]$ (**4**), and $(C_4H_9)_4N[Ir(2\text{-(3,5-difluorophenyl)-4-dimethylaminopyridine})_2\text{-}(CN)_2]$ (**5**) were synthesized and characterized using NMR, UV–vis absorption, and emission spectroscopy and electrochemical methods. In these complexes color and quantum yield tuning aspects are demonstrated by modulating the ligands with substituting donor and acceptor groups on both the pyridine and phenyl moieties of 2-phenylpyridine. Complexes **1**–**5** display intense photoluminescence maxima in the blue region of the visible spectrum and exhibit very high phosphorescence quantum yields, in the range of 50–80%, with excited-state lifetimes of 1–4 μs in acetonitrile solution at 298 K. DFT and time dependent-DFT calculations were performed on the ground and excited states of the investigated complexes to provide insight into the structural, electronic, and optical properties of these systems.

Introduction

Iridium(III) cyclometalated complexes are attracting widespread interest because of their unique photophysical properties and applications in organic light-emitting diodes (OLEDs).[1−4] The main requirements for OLEDs are that the phosphorescent emitter should have sharp colors in the blue, green, and red region and exhibit very high phosphorescence quantum yields. Even though there are several iridium complexes that exhibit green and red phosphorescence colors, blue-emitting iridium complexes, particularly in the deep blue region, are still scarce. Thus, the design and development of blue-light-emitting iridium complexes is a highly desirable and pursued task.[4−7] In principle, to blue-shift the emission in iridium(III) complexes can be realized by properly choosing substituents on the 2-phenylpyridine ligands or on the bipyridine (or phenanthroline) which stabilize the HOMO and/or destabilize the LUMO, thus increasing the HOMO−LUMO gap.[8,9] This strategy has been chosen by Slinker et al., who used fluorinated 2-phenylpyridine ligands to obtain iridium cationic complexes that show green-blue and green electroluminescence.[10] In these complexes the increase in the HOMO−LUMO gap with respect to complexes without

* To whom correspondence should be addressed. E-mail: mdkhaja.nazeeruddin@epfl.ch (M.K.N.); simona@thch.unipg.it (S.F.).
† Swiss Federal Institute of Technology.
‡ ISTM-CNR Perugia.
§ University of Valencia.

(1) Adachi, C.; Baldo, M. A.; Forrest, S. R.; Thompson, M. E. *Appl. Phys. Lett.* **2000**, *77*.
(2) Baldo, M. A.; Lamansky, S.; Burrows, P. E.; Thompson, M. E.; Forrest, S. R. *Appl. Phys. Lett.* **1999**, *75*, 4.
(3) Ikai, M.; Tokito, S.; Sakamoto, Y.; Suzuki, T.; Taga, Y. *Appl. Phys. Lett.* **2001**, *79*, 156.
(4) Nazeeruddin, M. K.; Humphry-Baker, R.; Berner, D.; Rivier, S.; Zuppiroli, L.; Grätzel, M. *J. Am. Chem. Soc.* **2003**, *125*, 8790−8797.
(5) Coppo, P.; Plummer, E. A.; De Cola, L. *Chem. Commun.* **2004**, 1774−1775.
(6) Lowry, M. S.; Hudson, W. R.; Pascal, R. A. J.; Bernhard, S. *J. Am. Chem. Soc.* **2004**, *126*, 14129.
(7) Lowry, M. S.; Goldsmith, J. I.; Slinker, J. D.; Rohl, R.; Pascal, R. A.; Malliaras, G. G.; Bernhard, S. *Chem. Mater.* **2005**, *17*, 5712.
(8) You, Y.; Park, S. Y. *J. Am. Chem. Soc.* **2005**, *127*, 12438−12439.
(9) Sajoto, T.; Djurovich, P. I.; Tamayo, A.; Yousufuddin, M.; Bau, R.; Thompson, M. E.; Holmes, R. H.; Forrest, S. R. *Inorg. Chem.* **2005**, *44*, 7992−8003.
(10) Slinker, J. D.; Gorodetsky, A. A.; Lowry, M. S.; Wang, J.; Parker, S.; Rohl, R.; Bernhard, S.; Malliaras, G. G. *J. Am. Chem. Soc.* **2004**, *126*, 2763.

10.1021/ic701814h CCC: $40.75
Published on Web 01/03/2008

fluorine substitution was due to stabilization of the HOMO.[11] We recently reported an iridium(III) complex where fluorine electron-acceptor substituents were used in 2-phenylpyridine ligands with the aim to stabilize the HOMO, coupled to dimethylamino electron-donating substituents on bipyridine, which have the role of destabilizing the LUMO; the result was an opening of the HOMO−LUMO gap, thus affording a green-blue light emitter.[12] An alternative approach has been used by Thompson et al., which consists of obtaining blue electroluminescence by stabilizing the HOMO of iridium cationic complexes using 1-phenylpyrazole ligand.[9]

Moreover, to be good candidates as phosphors in applications for OLED, cyclometalated iridium(III) complexes have to show very high quantum yields. Cyclometalated iridium complexes are known to have highest triplet quantum yields due to several factors:[13,14] (a) Iridium has large d-orbital splitting compared to other metals in the series. (b) Strong ligand field strength of phenyl anion ligand that increases the energy between t_{2g} and e_g orbitals, leading to enhanced gap between the e_g and LUMO of the ligand. (c) Close-lying $\pi-\pi^*$ and MLCT states together with the heavy atom effect that enhances the spin−orbit coupling. The even more effective strategy to magnify the quantum yields of this class of complexes is to increase further the gap between the e_g and LUMO orbitals by introducing ligands such as CN^-, which are known to have strong ligand field stabilization energy.[4] In such complexes, the charge-transfer excited states decay therefore mainly through radiative pathways.

Fine-tuning of phosphorescence wavelength in the blue region of the spectrum and enhancing phosphorescent quantum yields in iridium complexes are attractive for both fundamental research and practical applications.[4,5,9,15−17] Therefore, herein we provide an interesting approach for tuning phosphorescence wavelength from 470 to 450 nm of anionic iridium complexes maintaining a high phosphorescence quantum yield. This has been realized modulating HOMO/LUMO levels through a meticulous selection of donor and acceptor groups on 2-phenylpyridine ligand. Here we report synthesis and characterization of anionic Ir(III) complexes: $[Ir(2\text{-phenylpyridine})_2(CN)_2]$ (**1**), $(C_4H_9)_4N[Ir(2\text{-phenyl})\text{-}4\text{-dimethylaminopyridine})_2(CN)_2]$ (**2**), $(C_4H_9)_4N[Ir(2\text{-}(2,4\text{-difluorophenyl})\text{-pyridine})_2(CN)_2]$ (**3**), $(C_4H_9)_4N[Ir(2\text{-}(2,4\text{-difluorophenyl})\text{-}4\text{-dimethylaminopyridine})_2(CN)_2]$ (**4**), and $(C_4H_9)_4N[Ir(2\text{-}(3,5\text{-difluorophenyl})\text{-}4\text{-dimethylaminopyridine})_2(CN)_2]$ (**5**).

Density functional theory (DFT) and time-dependent DFT (TDDFT) calculations were performed to investigate in detail the electronic effect of the substituents on 2-phenylpyridine ligands and to provide insights on the excited states involved on the absorption and emission processes. TDDFT excited-state calculations on iridium(III) complexes are becoming increasingly popular,[10,12,15,18−23] the first paper in the subject being the work by Hay[18] on the neutral $[Ir(ppy)_3]$ complex. In this work we characterized the lowest singlet and triplet excited states of all the investigated complexes which can be related to the absorption and emission processes, respectively. These TDDFT results allow us to rationalize the effect of the substituent on the optical properties and to assign the nature of the relevant excited states in this class of compounds.

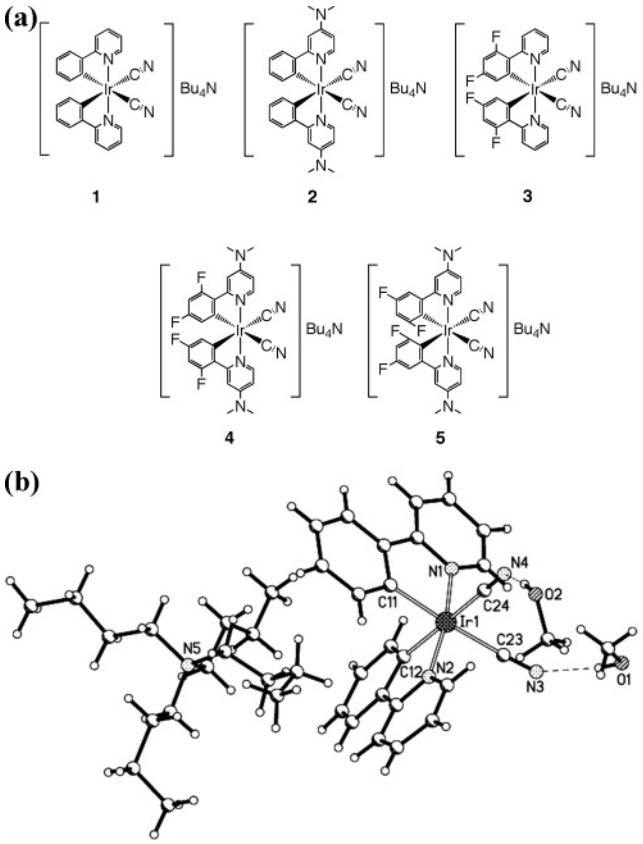

Figure 1. (a) Chemical structures of anionic iridium complexes **1**−**5**. (b) Crystal structure of $(C_4H_9)_4N[Ir(2\text{-phenylpyridine})_2(CN)_2]$.

Results and Discussion

1−**5** were conveniently synthesized in the low-boiling solvent dichloromethane by reacting the corresponding dichloro-bridged iridium(III) dimer with tetrabutylammonium cyanide (see Figure 1a for structures). The complexes were recrystallized from an ethanol/petroleum ether mixture and characterized by analytical and spectroscopic techniques. The

(11) Lowry, M. S.; Hudson, W. R.; Pascal, J. R. A.; Bernhard, S. *J. Am. Chem. Soc.* **2005**, *126*, 14129.
(12) De Angelis, F.; Fantacci, S.; Evans, N.; Klein, C.; Zakeeruddin, S. M.; Moser, J. E.; Kalyanasundaram, K.; Bolink, H. J.; Graetzel, M.; Nazeeruddin, M. K. *Inorg. Chem.* **2007**, *46*, 5989−6001.
(13) Ohsawa, Y.; Sprouse, S.; King, K. A.; DeArmond, M. K.; Hanck, K. W.; Watts, R. J. *J. Phys. Chem.* **1987**, *91*, 1047.
(14) Garces, F. O.; King, K. A.; Watts, R. J. *Inorg. Chem.* **1988**, *27*, 3464.
(15) Yang., C.-H.; Li., S.-W.; Chi., Y.; Cheng., Y.-M.; Yeh., Y.-S.; Chou., P.-T.; Lee., G.-H. *Inorg. Chem.* **2005**, *44*, 7770−7780.
(16) Lowry, M. S.; Hudson, W. R.; Pascal, J. R. A.; Bernhard, S. *J. Am. Chem. Soc.* **2005**, *126*, 14129.
(17) You, Y.; Park, S. Y. *J. Am. Chem. Soc.* **2005**, *127*, 12438−12439.
(18) Hay, P. J. *J. Phys. Chem. B* **2002**, *106*, 1634−1641.
(19) Polson, M.; Ravaglia, M.; Fracasso, S.; Garavelli, M.; Scandola, F. *Inorg. Chem.* **2004**, *44*, 1282−1289.
(20) Polson, M.; Ravaglia, M.; Fracasso, S.; Garavelli, M.; Scandola, F. *Inorg. Chem.* **2005**, *44*, 1282.
(21) Yang, C. H.; Su, W. L.; Fang, K. H.; Wang, S. P.; Sun, I. W. *Organometallics* **2006**, *25*, 4514.
(22) Obara, S.; Itabashi, M.; Okuda, F.; Tamaki, S.; Tanabe, Y.; Ishii, Y.; Nozaki, K.; Haga, M. *Inorg. Chem.* **2006**, *45*, 8907.
(23) Avilov, I.; Minoofar, P.; Comil, J.; De Cola, L. *J. Am. Chem. Soc.* **2007**, *129*, 8247.

Table 1. Absorption, Emission, Quantum Yields, Lifetimes, Radiative and Nonradiative Decay Rates, and Electrochemical Data of Complexes **1**−**5** Measured at 298 K in Dichloromethane Solution

complex	absorption, λ (nm) [$\epsilon/10^4$ M^{-1} cm^{-1}]	emission at 298 K[a]	quantum yields Φ_f	lifetime (μs)[b]	k_r (10^5 s^{-1})	k_{nr} (10^5 s^{-1})	electrochemical data V vs Fc	
							$E^{1/2}_{ox}$	$E^{1/2}_{red}$
1	260 (41.7), 337 (0.85), 384 (0.58), 433_{sh} (0.61)	470, 508, 542sh	0.75 ± 0.1	3.26 ± 0.03 (45 ns)	2.30 ± 0.3	0.76 ± 0.3	0.55	−2.69
2	272 (3.79), 302 sh (2.21), 3.32 (1.07), 354 (0.89), 380 (0.59)	465, 488, 525 sh	0.54 ± 0.1	1.82 ± 0.03 (26 ns)	2.97 ± 0.6	2.53 ± 0.6	0.33	−3.0
3	254 (6.04), 290 (2.79), 362 (0.78), 390 (0.38)	460, 485	0.80 ± 0.1	3.28 ± 0.03 (32 ns)	2.44 ± 0.3	0.61 ± 0.3	0.96	−2.6
4	266 (2.83), 290 (2.63), 302 (2.38), 338 (1.32), 360 (1.08)	451, 471, 525 sh	0.62 ± 0.1	1.30 ± 0.03 (134 ns)	4.77 ± 0.9	2.92 ± 0.9	0.58	−2.98
5	268 (5.25), 288 (4.20), 302sh (3.22), 356 (1.52), 378 (0.95)	468, 492	0.64 ± 0.1	3.00 ± 0.03 (33 ns)	2.13 ± 0.3	1.20 ± 0.3	0.53	−2.80

[a] The emission spectra were obtained from degassed solutions by exciting into the lowest MLCT band. The maxima were extrapolated from deconvoluting the emission spectra and the details are given in the Supporting Information. [b] Values in parenthesis are aerated solutions.

crystal structure of complex **1** clearly shows that the cyanide ligands are coordinating through the carbon atom and adopt a cis configuration (see Figure 1b).

The cyclic voltammogram of complex **1** measured in acetonitrile containing 0.1 M tetrabutylammonium hexafluorophosphate with a 0.1 V scan rate show a quasi-reversible couple at 0.55 V/s vs ferrocene (Fc) due to iridium(III/IV). Upon scanning cathodically, a reversible reduction wave at −2.69 V vs Fc is observed that is assigned to the reduction 2-phenylpyridine. It is interesting to note that, in complex **2**, the ligand-based reduction potential (−3.0 V vs Fc) and the iridium oxidation potential (0.33 V vs Fc) shifted cathodically by 0.310 and 0.220 V, respectively, compared to complex **1**, demonstrating the extent of destabilization of LUMO and HOMO orbitals caused by 4-dimethylamino group. On the other hand, in complex **3**, the iridium oxidation potential (0.96 V vs Fc), shifted anodically by 0.41 V compared to complex **1**. The increase in the HOMO−LUMO gap of complex **3** with respect to complex **1** is mainly due to stabilization of the HOMO orbitals, while in the case of complex **2**, destabilisation of the LUMO results in no significant difference in the emission maxima of complexes **2** and **3**. This is not surprising since substitution of donor or acceptor groups tunes both the HOMOs and the LUMOs in parallel, leading to marginal changes in the photophysical properties.

To overcome the above disadvantage, we have synthesized complex **4** by using a ligand that contains a donor group on the pyridine and acceptor groups on the phenyl ring. The cyclic voltammogram of the complex **4** shows a quasi-reversible wave at 0.58 V and a reduction wave at −2.98 vs Fc, which are due to oxidation of Ir(III/IV) and reduction of 2-(2,4-difluorophenyl)-4-dimethylaminopyridine, respectively (Table 1). The reduction potential of complex **4** is shifted cathodically by 0.29 V compared to that of complex **1**, demonstrating the extent of destabilization of the LUMO in complex **4**. Substitution of the donor dimethylamino group not only destabilizes the LUMO but also the HOMO. However, the destabilization of the iridium-based HOMO caused by the 4-dimethylamino donor group is overcome by the presence of electron-acceptor fluoride groups on phenyl in complex **4**, thus ensuing a net increase in the gap between the HOMO and the LUMO of **4** compared to the complexes **2** and **3**. (Table 1).[10]

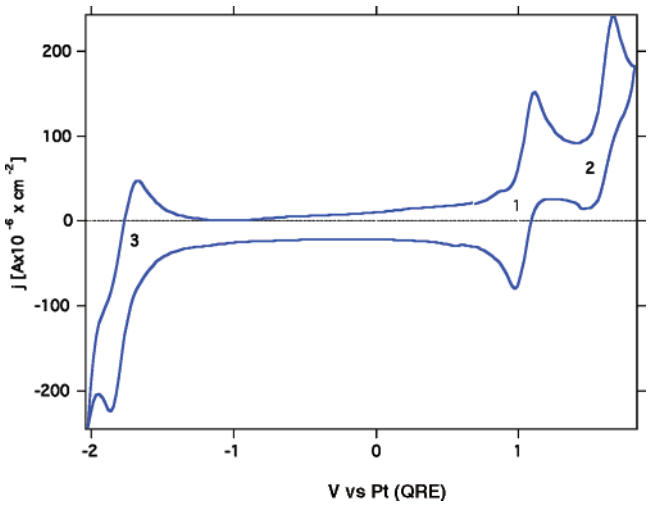

Figure 2. Cyclic voltammogram of complex **5** measured in acetonitrile in the presence of 0.1 M tetrabutylammonium hexafluorophosphate as supporting electrolyte with 100 mV/s scan speed. The redox couple labeled as 1 is due to ferrocene/ferrocenium, which is used as an internal standard; 2 is Ir(III/VI); 3 is ligand reduction. The direction of the measurement is from positive to negative.

The difference between complexes **4** and **5** is only in the position of the fluoride atoms on the phenyl of the 2-phenylpyridine ligand, which are at 2,4-position in the former and 3,5-position in the later. The complex **5** oxidation potential shifted 0.05 V cathodically and the reduction potential by 0.18 V anodically compared to complex **4** (Figure 2) thus making the HOMO−LUMO gap smaller compared to complex **4**, signifying the influence of position of the substituents. One possible explanation for this quite unexpected electrochemical shift of the complex **5** compared to the complex **4** is that the fluorides in the 3,5-position lowers the LUMO, thereby decreasing the HOMO−LUMO gap compared to complex **4**.

Figure 3 shows representative absorption and emission spectra of complex **4** measured in dichloromethane solution

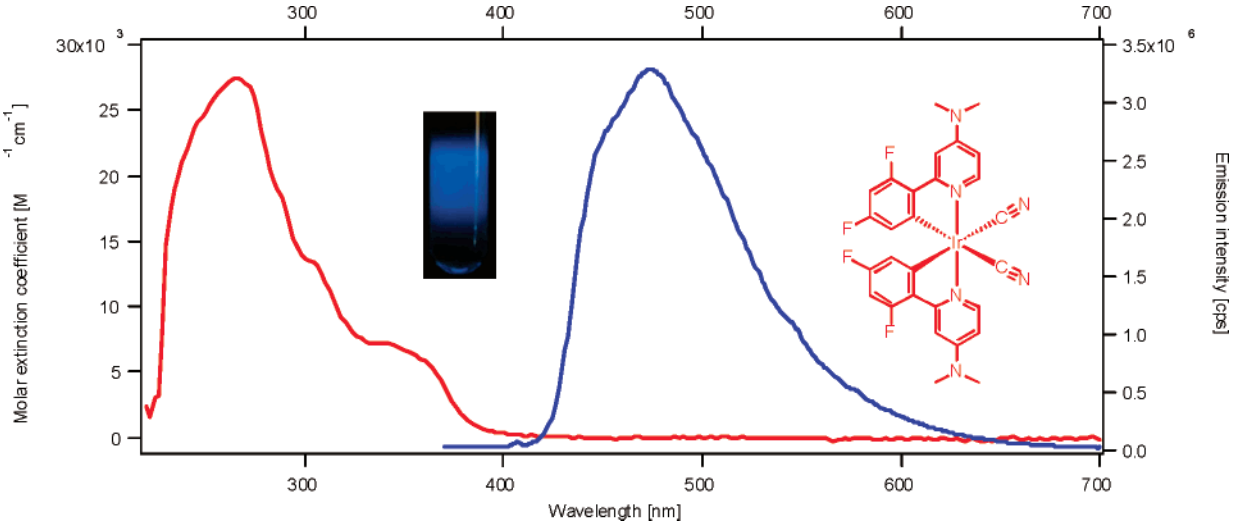

Figure 3. Absorption (red line) and emission (blue line) spectra of $(C_4H_9)_4N[Ir(2,4\text{-difluorophenyl-4-dimethylaminopyridine})_2(CN)]_2$ (**4**) in dichloromethane solution at 298 K. The inserts show a photo of the **4** solution exhibiting very strong blue emission upon excitation at 380 nm and the chemical structure of the complex **4**.

at 298 K. The complex displays bands in the UV and the visible regions due to intraligand ($\pi-\pi^*$) and metal-to-ligand charge-transfer transitions (MLCT), respectively (Table 1).[24] Complexes **1**−**4** upon excitation at 380 nm show emission maxima in the blue region; complex **5** exhibits a 21 nm red-shift compared to complex **4**. The air-equilibrated dichloromethane solutions exhibit shorter luminescence lifetimes (70−90 ns) compared to the degassed solutions (1−3 μs). When excited within the $\pi-\pi^*$ and MLCT absorption bands of complex **4** at 298 K, emission maxima at 451 nm, due to the 2,4-difluorophenyl-4-dimethylaminopyridine ligand that increases the gap between LUMO and HOMO resulting in a blue shift of the emission maxima compared to the complexes **1**−**3**, are visible. It is apparent from the Figure 3 that the complex **4** shows brilliant blue color, unravelling the tuning aspect of the HOMO and the LUMO levels. The complex **5** emission maxima are significantly red-shifted compared to complex **4**, demonstrating the influence of position of the substitution effect on photophysical properties.

From the quantum yield, Φ, and the lifetime, τ, values, assuming a unitary intersystem crossing efficiency, the radiative and overall nonradiative rate constants k_r and k_{nr} were calculated for the series of complexes through the equations $k_r = \Phi/\tau$ and $k_{nr} = (1 - \Phi)/\tau$[25] (see Table 1). As it appears from Table 1, k_r values show comparable values in the investigated series of complexes: considering the experimental uncertainty in the quantum yields and the fact that k_r values should increase as the third power of the emission frequency, according to the Einstein law of spontaneous emission,[26,27] the measured k_r values, which increase with increasing the emission frequency, involve similar transition dipole moments for the emitting transition and are therefore suggestive of a common chromophoric basis of the emitting excited states. On the other hand, k_{nr} values show larger variability compared to k_r values. In particular, for complexes **1**−**4**, a trend can be outlined. Complexes **1** and **3** show similarly low k_{nr} values, while complexes **2** and **4** show similarly high values, ca. 3−4 times larger than k_{nr} values for complexes **1** and **3**. Therefore, introduction of 4-dimethylaminopyridine in **2** and **4** is found to lead to increased k_{nr} values, which in turn leads to a reduction of the overall quantum yield. This might be due to the presence of low-frequency vibrational modes associated to the dimethylaminopyridine moiety which allow the excited-state to perform wide-amplitude motions, thus sampling more effectively nonradiative deactivation pathways.[12] Introduction of fluoride substituents in the 2,4-positions on the other hand does not substantially influence the quantum yields, apart from a slight increase and decrease of k_r and k_{nr} values, respectively, in line with the increased emission energy observed going from **1** to **3**.[25,28−30] Complex **5** shows smaller k_r and k_{nr} values compared with those observed for **4**, suggesting that the position of the fluoride substituents can significantly influence both radiative and nonradiative deactivation pathways.

It is worth noting that the argon-degassed dichloromethane solution of the complex **4** shows bright blue luminescence in a lighted room and displays very high phosphorescence quantum yields, 62% ± 10%, in solution at room temperature. The emission decayed as a single exponential with lifetimes of 1.3 μs in degassed CH_2Cl_2 solution where the origin of the emitting state is the same.[31] The quantum yield data of complexes **1**−**5** are measured using recrystallized quinine sulfate in 1 N H_2SO_4 as a quantum yield standard. At the same time, a widely referred sample $Ru(bpy)_3PF_6$ was used as a secondary standard to verify the yields obtained with quinine sulfate. The data obtained using both the

(24) Schmid, B.; Garces, F. O.; Watts, R. J. *Inorg. Chem.* **1994**, *33*, 9.
(25) Kober, E. M.; Caspar, J. V.; Lumpkin, R. S.; Meyer, T. J. *J. Phys. Chem.* **1986**, *90*, 3722.
(26) Strickler, S. J.; Berg, R. A. J. *J. Chem. Phys.* **1962**, *37*, 814.
(27) Einstein, A. *Phys. Z.* **1917**, *18*, 121.
(28) Freed, K. F.; Jortner, J. *J. Chem. Phys* **1970**, *52*, 6272.
(29) Bixon, M.; Jortner, J. *J. Chem. Phys.* **1968**, *48*, 715.
(30) Henry, B. R.; Siebrand, W. *Organic Molecular Photophysics*; Wiley: New York, 1973.
(31) Ichimura, K.; Kobayashi, T.; King, K. A.; Watts, R. J. *J. Phys. Chem.* **1987**, *91*, 6104.

Table 2. Emission and Lifetime Data of Complexes **1**, **2**, and **4** in Various Solvents

complex	solvent[a]	emission λ max. at 298 K	lifetime[b] τ (ns)$_{air}$	lifetime[b] τ (μs)$_{argon}$
1	CH_3OH	467, 497, 535sh	84	4.00
	CH_2Cl_2	470, 508, 542sh	45	3.26
	CH_3CN	477, 505, 547sh	38	2.52
	CH_3OCH_3	481, 510, 546	28	2.82
	THF	481, 508, 547sh	28	2.75
2	CH_3OH	456, 482, 518	30	4.95
	CH_2Cl_2	465, 488, 525 sh	26	1.82
	CH_3CN	466, 492, 524	28	1.70
	CH_3OCH_3	472, 497, 528 sh	32	3.44
	THF	475, 498, 522 sh	22	1.90
4	CH_3OH	435, 464, 491	30	4.95
	CH_2Cl_2	451, 471, 525 sh	134	1.30
	CH_3CN	449, 472, 505	28	1.70
	CH_3OCH_3	450, 470, 522 sh	32	3.44
	THF	449, 477, 506 sh	22	1.90

[a] THF = tetrahydrofuran. [b] Emission data were collected at 298 K using fresh solutions. Pulsed excitation at 450 nm was provided by a Q-switched, frequency tripled, Nd:YAG laser pumping an optical parametric oscillator (OPO). The pulse duration was 5 ns and the repetition rate was 30 Hz. The solutions were degassed by Ar bubbling for 10 min.

standards are in excellent agreement and indeed show yields in the range 50−80%.

Table 2 lists luminescence maxima and lifetimes for select complexes **1**, **2**, and **4** measured at 278 K, in various protic and aprotic solvents. The emission spectra for complexes **1**, **2**, and **4** show solvatochromism, and the data demonstrate that the emission maximum is blue-shifted and the lifetime increased going from aprotic solvent to protic solvents. The solvatochromism of absorption and emission spectra has been observed for analogous Ru(II) d^6 cyano complexes.[32] The ≈15 nm blue-shift of emission maxima in methanol compared to aprotic solvents is probably due to hydrogen bonding to the cyanide group, which further stabilizes the HOMO compared, resulting in an increased HOMO−LUMO gap.[32] A similar influence of the solvent on the emission properties has been reported by Timpson et al. for Ru−cyano complexes.[32g] The measured lifetimes increased significantly in degassed solutions compared to aerated solutions due to quenching of the intense emission from the MLCT excited-state to the ground state triplet oxygen by energy transfer.

DFT/TDDFT Results. We optimized molecular structures of **1**−**5** complexes and compared them with X-ray data for complex **1**. The main computed geometrical parameters are reported in the Supporting Information. In agreement with X-ray data, we find that the CN ligands are bound through the C end to the metal center. For complex **1**, Ir−N and Ir−C (ppy) distances of 2.046 and 2.051 Å are calculated, which nicely compare to experimental values of 2.061−2.063 and 2.059−2.055 Å, respectively. Ir−C (CN) distances of 2.060 Å are computed to be compared to experimental values of 2.066−2.079 Å. Bond angles are also accurately reproduced, apart from ∠C−Ir−C (ppy), which is overestimated by ca. 5°. This deviation is probably due to the presence of a TBA counterion in the crystal structure lying at the side of the phenyl rings.

In Figure 4 we report a schematic representation of the molecular orbital energies of complexes **1**−**5**, while in Figure 5 isodensity plots of relevant molecular orbitals for **1** and **2** are reported.

The HOMO of complex **1** is an Ir(t_{2g}) orbital combined in an antibonding fashion with the phenyl carbon π orbitals of the ppy ligands. The HOMO is followed, in order of decreasing energy, by two almost degenerate orbitals showing a large contribution from Ir(t_{2g}) states with small percentages coming from the ppy and CN ligands, while the HOMO-3 is mainly a π bonding combination of the ppy ligand with small metal character, see Figure 5a. The two LUMOs of complex **1** are a degenerate couple of π^* character delocalized on both the phenyl and pyridine moieties of the ppy ligands. At higher energies two almost degenerate orbitals (LUMO+2/LUMO+3) of π^* character, localized on the pyridine moieties of ppy, are found. The corresponding phenyl π^* orbitals (LUMO+4/LUMO+5) are found still at higher energies. We notice that the Ir(e_g) d_{z^2} and $d_{x^2-y^2}$ orbitals lie still at higher energy, being the LUMO+8 and LUMO+9 (not shown). The molecular orbitals of complex **3** are qualitatively similar to those of complex **1**. For the dimethylamino-substituted complexes **2**, **4**, and **5**, two orbitals showing sizable contributions from the dimethylamino N lone pairs insert among the HOMOs. For all the investigated complexes, the same LUMO pattern is calculated, apart from the fact that complexes **2**, **4**, and **5** show a small contribution from the dimethylamino N lone pairs in the LUMO+2/LUMO+3, compare Figure 5a and b.

To gain insight into the absorption and emission processes of the investigated complexes, we analyzed the 10 lowest singlet−singlet and singlet−triplet excitations calculated at both the ground state singlet S_0 and lowest excited triplet state T_1 optimized geometries. The energy and character, see Computational Details, of the relevant excited states are reported in Table 3. The absorption spectra of the investigated complexes show similar features, with the low-energy spectral region being dominated by transitions of main MLCT character, while at higher energy, transitions of main $\pi-\pi^*$ character are found. Here we only briefly describe the absorption spectrum of complex **1** and discuss the differences between **4** and **5**. At its ground-state geometry, the lowest TDDFT excited states of **1** are calculated to be of triplet character at 442 and 439 nm, essentially corresponding to HOMO−LUMO and HOMO−LUMO+1 MLCT transitions. The calculated transitions nicely correlate with the band tail extending into the visible region of the experimental absorption spectrum, suggesting that this feature is related to spin-forbidden singlet−triplet transitions which become allowed due to the strong spin−orbit coupling of

(32) (a) Demas, J. N.; Turner, T. F.; Crosby, G. A. *Inorg. Chem.* **1969**, *8*, 674. (b) Sullivan, B. P.; Calvert, J. M.; Meyer, T. J. *Inorg. Chem.* **1980**, *19*, 1404. (c) Bignozzi, C. A.; Scandola, F. *Inorg. Chem.* **1984**, *23*, 1540. (d) Bignozzi, C. A.; Chiorboli, C.; Indelli, M. A.; Rampi, Scandola, M. A.; Varani, G.; Scandola, F. *J. Am. Chem. Soc.* **1986**, *108*, 7872. (e) Kitamura, N.; Kim, H.-B.; Kawanishy, Y.; Obata, R.; Tazuke, S. *J. Phys. Chem.* **1986**, *90*, 3722. (f) Fung, E. Y.; Chua, A. C. M.; Curtis, J. C. *Inorg. Chem.* **1988**, *27*, 1294. (g) Timpson, C. J.; Bignozzi, C. A.; Sullivan, B. P.; Kober, E. M.; Meyer, T. J. *J. Phys. Chem.* **1996**, *100*, 2915.

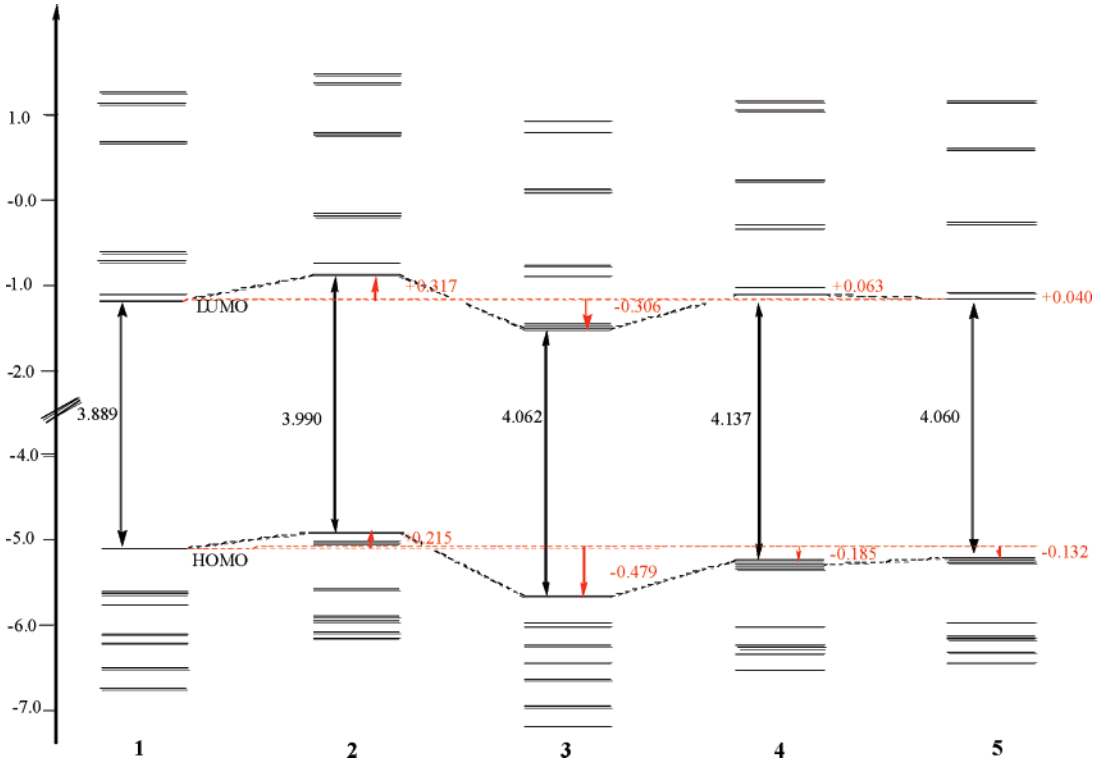

Figure 4. Schematic representation of the frontier orbitals of complexes **1**−**5**.

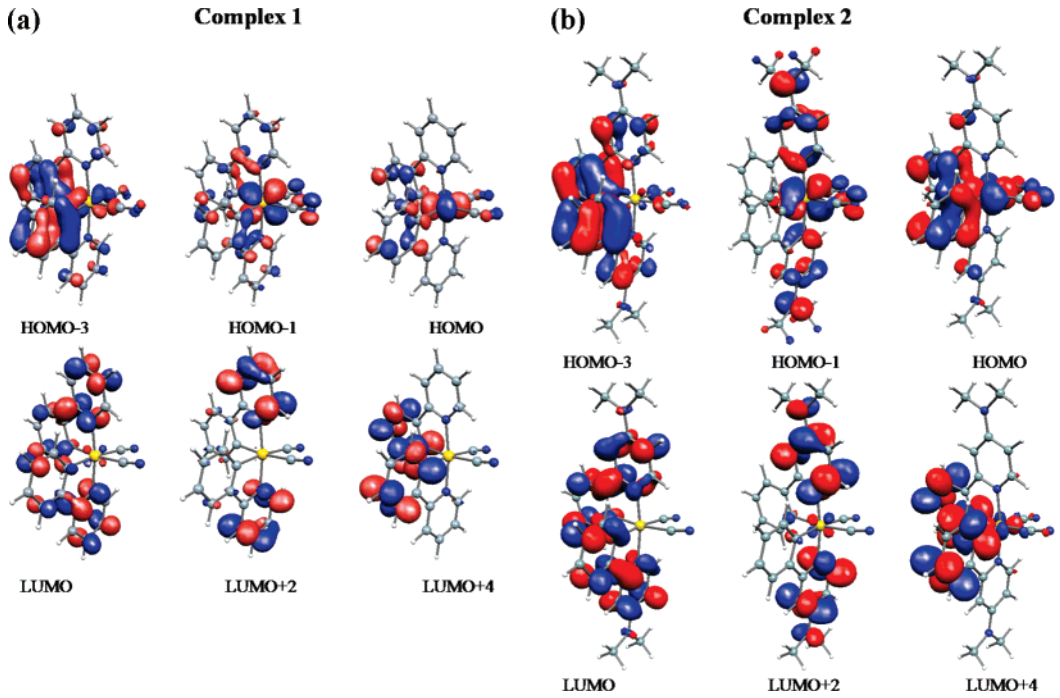

Figure 5. (a) Isodensity plots of the frontier orbitals of complex **1**. Isodensity value 0.03. (b) Isodensity plots of the frontier orbitals of complex **2**. Isodensity value 0.03.

the Ir(III) center. The lowest singlet excited-state is calculated to give rise to quite an intense HOMO−LUMO transition at 396 nm (f = 0.057), followed at higher energy by an intense HOMO-1/HOMO-2−LUMO/LUMO+1 transition at 332 nm (f = 0.196), with still at higher energy a HOMO-3−LUMO+1 transition of relevant intensity (f = 0.099) calculated at 312 nm. The 396 and 332 nm transitions are therefore assigned as having MLCT character, in good agreement with experimental values of 384 and 337 nm. The 312 nm transition essentially corresponds to a $\pi-\pi^*$ excitation within the phenylpyridine ligand therefore belonging to the $\pi-\pi^*$ manifold extending into the UV region. The main difference between the low-energy portion of the absorption spectra of **4** and **5** is a red-shift of the MLCT feature in **5** compared to **4**. This trend is nicely reproduced by our calculations, which show for **5** a lowest singlet−singlet

Table 3. Calculated Lowest Singlet−Triplet and Singlet−Singlet Transitions (nm, $f > 0.04$) Related to the Absorption Spectra in Dichloromethane Solution for Complexes **1**−**5**, Comparison between Calculated Lowest Singlet−Triplet Transitions (nm) Related to Emission and Experimental High-Energy Emission Features for Complexes **1**−**5** in Dichloromethane Solution, and Emission Assignment and Composition of the Emitting Excited State in Terms of Single Orbital Excitations[a]

Absorption					
	1	**2**	**3**	**4**	**5**
S_0-T_1	442	424	424	413	422
S_0-T_2	439	419	422	413	420
S_0-S_n	$n = 1$	$n = 1$	$n = 1$	$n = 1$	$n = 1$
	396 (0.057)	377 (0.121)	375 (0.049)	354 (0.066)	364 (0.042)
S_0-S_n	$n = 6$	$n = 3$	$n = 5$	$n = 2$	$n = 2$
	330 (0.196)	357 (0.059)	326(0.171)	352 (0.127)	359 (0.150)
S_0-S_n	$n = 10$	$n = 5$	$n = 10$	$n = 5$	$n = 5$
	312 (0.099)	345 (0.080)	297 (0.114)	342 (0.111)	350 (0.070)
S_0-S_n	−	$n = 10$	−	$n = 7$	−
		298 (0.136)		293 (0.050)	
S_0-S_n	−	−	−	$n = 9$	−
				289 (0.205)	

Emission					
	1	**2**	**3**	**4**	**5**
exptl	470	465	460	451	468
S_0-T_1	480	470	454	440	465
character	^{3}MLCT	^{3}MLCT/$\pi-\pi^*$	^{3}MLCT	^{3}MLCT/$\pi-\pi^*$	^{3}MLCT/$\pi-\pi^*$
	79%(H → L)	85%(H → L)	61%(H → L)	38%(H → L)	75%(H → L)
		12%(H-3 → L+1)			
	14%(H-1 → L+1)		21%(H-1 → L+1)	24% (H-1 → L+1)	15% (H-3 → L+1)
				18%(H-2 → L)	
				14%(H-3 → L+1)	

[a] For singlet−triplet transitions, oscillator strengths are zero because of the neglect of spin−orbit coupling in the TDDFT calculations.

excitation of MLCT character at 364 nm, to be compared to the 355 nm value calculated for **4**. The calculated transitions are in excellent agreement with the experimental values of 378 and 360 nm for **5** and **4**, respectively; this red-shift appears to be related to the decreased HOMO−LUMO gap calculated for **5** compared to **4**, confirming the relevant effect of the position of the F substituents on the cyclometalating ligand. We finally remark that having in mind the electronic structure picture of complexes **1**−**5** discussed above and considering the mixed Ir(t_{2g})−ppy(π) character of the HOMOs, MLCT transitions actually show in all cases a sizable amount of mixing with $\pi-\pi^*$ excitations of the phenylpyridine ligands.

Comparison of excitation energies at the triplet excited-state geometry with emission spectral maxima is not straightforward since the emission intensities are determined, for a given couple of electronic states, by vibrational wavefunction overlaps (the Franck−Condon factors) between the excited-state lowest vibrational level and the various vibrational levels of the ground state. The computation of Franck−Condon factors of large molecules in solution, including geometry optimization of the excited states, has been recently achieved.[33,34] Such a procedure would probably allow us to perform a more direct comparison between calculated and experimental data. Nevertheless, the computed lowest singlet−triplet transitions for the investigated anionic complexes are in excellent agreement with experimental values reported in Table 1, reproducing the blue-shift observed going from complex **1** to complex **4**. In particular, we compare in Table 3 the high-energy feature of the emission spectrum with the lowest calculated triplet excitation energy. As can be noticed, the calculated values follow the experimental trend, showing an almost quantitative agreement with experimental values. From the analysis of the TDDFT eigenvectors calculated at the T_1 geometries, we can assign the character of the electronic emitting state for **1**−**4** complexes. For complex **1**, the S_0-T_1 transition shows two main contributions, see Table 3, having MLCT character from the Ir($t_{2g}-d_{xy}$/$t_{2g}-d_{xz}$)−ppy(π) levels to the ppy (π^*) framework. Increased mixing between MLCT and $\pi-\pi^*$ character is computed for complex **2**, the S_0-T_1 transition showing a sizable contribution from (HOMO-3 → LUMO+1). The emitting state of complex **3** has similar character to that computed for complex **1**, even though the weight of the two contributing excitations slightly changes, see Table 3. For complex **4**, the S_0-T_1 transition is, as in **2**, of mixed MLCT and $\pi-\pi^*$ character, showing contributions from all the three Ir(t_{2g}) orbitals plus the $\pi-\pi^*$ component (HOMO-3 → LUMO+1). These results therefore confirm the common nature of the excited states inferred from the photophysical properties, with complexes **2** and **4**, bearing a dimethylamino functionalized ppy ligand, showing also contributions to the emitting excited-state arising from the NMe_2 lone pairs. This is possibly related, as mentioned above, to the increased nonradiative rate constants measured for species **2** and **4**, which ultimately leads to decreased quantum yields for these species compared to **1** and **3**.

(33) Scalmani, G.; Frisch, M. J.; Mennucci, B.; Tomasi, J.; Barone, V. J. *Chem. Phys.* **2006**, *124*, 094107.
(34) Santoro, F.; Improta, R.; Lami, A.; Bloino, J.; Barone, V. J. *Chem. Phys.* **2007**, *126*, 084509.

Experimental Section

Materials and Methods. The solvents (puriss grade) were purchased from Fluka. 2-Phenylpyridine ligand and hydrated iridium trichloride were used as received from Aldrich and Johnson Matthey, respectively. The dichlorobridged iridium dimer $[Ir(ppy)_2(Cl)]_2$,[14] $[Ir(dfppy)_2(Cl)]_2$, and 2-(4,6-difluorophenyl)pyridine[35] were synthesized using a reported procedure.

ESI (electrospray ionization) experiments were conducted with a Thermo Finnigan Advantage Max Ion trap spectrometer in negative ion acquiring mode; sheath gas flow rate was set at 25 (arbitrary unit), auxiliary gas flow rate at 5 (arbitrary unit), spray voltage at 3.25 (kV), capillary temperature at 270 °C. UV−vis spectra were recorded in a 1 cm path length quartz cell on a Cary 5 spectrophotometer. Emission spectra were recorded on a Spex Fluorolog 112 using a 90° optical geometry. The emitted light was detected with a Hamamatsu R2658 photomultiplier operated in single photon counting mode. The emission spectra were photometrically corrected using a NBS calibrated 200W tungsten lamp as reference source. The quantum yields were determined using the following equation:[36,37]

$$\phi_X = \phi r K_{\text{opt}} \frac{(D/A_{\text{exc}})_X}{(D/A_{\text{exc}})_r}$$

Where the subscript *X* denotes the substance whose quantum yield is determined and r is the reference substance quininesulfate (3×10^{-5} M in 1 M H_2SO_4), whose luminescence quantum yield is assumed to be 0.545;[37] K_{opt} is the optical factor referring to the higher refractive index of the dichloromethane ($n_D = 1.424$) compared to the water solution ($n_D = 1.333$); *D* is the integrated area under the emission spectrum; A_{exc} is the absorbance at the exciting wavelength. A secondary standard using recrystallized $Ru(bpy)_3PF_6$ solution was also employed to verify the yields. Emission lifetimes were measured using a pulsed Nd-laser photolysis set up that is based on a Nd:YAG oscillator pumping a Nd-glass laser system in line. In addition to doubled and tripled frequenciese (530 and 353 nm) laser pulses at additional wavelengths for excitation were generated by passing the Nd laser pules through an OPA. The emission decay was followed on a Tektronix DSA 640 digitizing signal analyzer, using a Hamamatsu R928 photomultiplier to convert the light signal to a voltage waveform. The solutions were prepared to give approximate concentrations of 0.1 μM.

Voltammetric measurements employed a PC-controlled AutoLab PSTAT10 electrochemical workstation. Cyclic voltammograms (CVs) were obtained at different scan rates using 0.1 M $TBAPF_6$ as supporting electrolyte in acetonitrile. In all cases a platinum foil and a platinum wire were employed as the counter and reference electrode, respectively. At the end of the each measurement the ferrocene/ferrocinium (Fc^+/Fc) potential is measured and use as an internal reference. ^{1}H and ^{13}C NMR spectra were measured with Bruker ACP-200 spectrometer at 200 MHz and 50.3 MHz, respectively. The reported chemical shifts were against TMS.

Synthesis and Characterization. 2-Iodo-4-dimethylaminopyridine. $BF_3{\cdot}Et_2O$ (8.4 g, 59 mmol) was added dropwise to a solution of 4-dimethylaminopyridine (6 g, 49 mmol) in dry THF (250 mL) at 0 °C. The resulting mixture was stirred 1 h at 0 °C under nitrogen. The temperature was cooled to −78 °C, and BuLi (1.6 M in hexane, 46 mL, 74 mmol) was added dropwise. The resulting mixture was stirred for 1 h at −78 °C, and a solution of I_2 (18.7 g, 74 mmol) in dry THF (50 mL) was added dropwise. The resulting mixture was stirred at −78 °C for 2 h and allowed to warm to room temperature (2 h). THF was evaporated, and a saturated $Na_2S_2O_5$ solution was added. The resulting slurry was extracted with EtOAc (5 × 150 mL). The combined organic fractions were successively washed with saturated $Na_2S_2O_5$ (50 mL), brine (50 mL), dried over $MgSO_4$, filtered, and evaporated to dryness. The resulting residue was purified by column chromatography (SiO_2, EtOAc/petroleum ether, 1:1) to afford 7 g (57%) of the desired compound as a colorless oil which solidified upon standing. ^{1}H and ^{13}C NMR data are in agreement with those reported in the literature.[38]

2-Phenyl-4-dimethylaminopyridine. A mixture of 2-iodo-4-dimethylaminopyridine (3.3 g, 13.3 mmol), phenylboronic acid (2.5 g, 20 mmol), and K_2CO_3 (8.3 g, 60 mmol) in toluene (60 mL) and water (10 mL) was degassed with nitrogen for 15 min. $Pd(PPh_3)_4$ (800 mg, 0.66 mmol) was added, and the resulting mixture was heated to 90 °C for 48 h under nitrogen. After being cooled to room temperature, the aqueous phase was separated and extracted with EtOAc (3 × 100 mL). The combined organic fractions were washed with brine, dried over $MgSO_4$, filtered, and evaporated to afford a brown oil. The following oil was dissolved in Et_2O and extracted with 10% HCl solution (3 × 50 mL). The combined aqueous fractions were washed with Et_2O (2 × 100 mL) and neutralized with concentrated NaOH solution. The resulting mixture was extracted with EtOAc (4 × 100 mL) and the combined organic fractions were washed with brine (50 mL), dried over $MgSO_4$, filtered, and evaporated to dryness. The obtained residue was then purified by column chromatography (SiO_2, CH_2Cl_2/MeOH, 97:3) to afford 1.2 g (46%) of the titled compound as a colorless oil which solidify upon standing. ^{1}H NMR ($CDCl_3$, 298K, 200 MHz, δ) 3.08 (s, 6H), 6.49 (dd, $J = 2.5$ and 6 Hz, 1H), 6.91 (s, 1H), 7.47 (m, 3H), 7.94 (d, $J = 7$ Hz 2H), 8.34 (d, $J = 6$ Hz, 1H). ^{13}C NMR ($CDCl_3$, 298K, 50 Hz, δ) 39.2, 103.6, 105.4, 127.0, 128.6, 132.2, 140.5, 149.5, 155.1, 157.8.

2-(2,4-Difluorophenyl)-4-dimethylaminopyridine. A mixture of 2-iodo-4-dimethylaminopyridine (3 g, 12 mmol), 2,4-difluorophenylboronic acid (2.3 g, 14.5 mmol), and K_2CO_3 (6 g, 43.5 mmol) in toluene (60 mL) and water (10 mL) was degassed with nitrogen for 15 min. $Pd(PPh_3)_4$ (800 mg, 0.66 mmol) was added, and the resulting mixture was heated to 90 °C for 48 h under nitrogen. After being cooled to room temperature, the aqueous phase was separated and extracted with EtOAc (3 × 100 mL). The combined organic fractions were washed with brine, dried over $MgSO_4$, filtered, and evaporated. The crude compound was purified by column chromatography (SiO_2, $CHCl_3$, then $CHCl_3$/MeOH, 97:3) to afford 2.2 g (78%) of the titled compound as a slightly yellow oil which solidify upon standing. If some impurities remain, the compound can be purified by following the acidic extraction followed by basic recovery as performed before for 2-phenyl-4-dimethylaminopyridine. ^{1}H NMR ($CDCl_3$, 298K, 200 MHz, δ) 3.05 (s, 6H), 6.49 (dd, $J = 2.5$ and 6 Hz, 1H), 6.92 (m, 3H), 7.94 (m, 1H), 8.33 (d, $J = 6$ Hz, 1H).

2-(3,5-Difluorophenyl)-4-dimethylaminopyridine. A mixture of 2-iodo-4-dimethylaminopyridine (2.68 g, 10.8 mmol), 3,5-difluorophenylboronic acid (2.56 g, 16.2 mmol), and K_2CO_3 (6.7 g, 48.6 mmol) in toluene (60 mL) and water (10 mL) was degassed with nitrogen for 15 min. $Pd(PPh_3)_4$ (800 mg, 0.66 mmol) was

(35) Lohse, O.; Thevenin, P.; Waldvogel, E. *Synlett* **1999**, *1*, 45.
(36) Parker, C. A. *Measurement of Fluorescence Efficiency*; Elsevier Publishing Co.: New York, 1968.
(37) Kartens, T.; Kobs, K. *J. Phys. Chem.* **1980**, *84*, 1871.
(38) Cuperly, D.; Gros, P.; Fort, Y. *J. Org. Chem.* **2002**, *67*, 238−241.

added, and the resulting mixture was heated to 90 °C for 48 h under nitrogen. After being cooled to room temperature, the aqueous phase was separated and extracted with EtOAc (3 × 100 mL). The combined organic fractions were washed with brine, dried over $MgSO_4$, filtered, and evaporated to afford a brown oil. The follwing oil was dissolved in Et_2O and extracted with 10% HCl solution (3 × 50 mL). The combined aqueous fractions were washed with Et_2O (2 × 100 mL) and neutralized with concentrated NaOH solution. The resulting mixture was extracted with EtOAc (4 × 100 mL), the combined organic fractions were washed with brine (50 mL), dried over $MgSO_4$, filtered, and evaporated to dryness. The obtained residue was then purified by column chromatography (SiO_2, EtOAc) to afford 1.2 g (46%) of the titled compound as a colorless oil which solidify upon standing. The crude compound was purified by column chromatography (SiO_2, $CHCl_3$ then $CHCl_3$/MeOH, 97:3) to afford 1 g (40%) of the titled compound as a colorless oil which solidify upon standing. ^{1}H NMR ($CDCl_3$, 298K, 200 MHz, δ) 3.08 (s, 6H), 6.51 (dd, J = 2.5 and 6 Hz, 1H), 6.82 (m, 2H), 7.49 (m, 2H), 8.32 (d, J = 6 Hz, 1H).

Synthesis of [(2-phenylpyridine)$_2$IrCl]$_2$, [(2-phenyl-4-dimethylaminopyridine)$_2$IrCl]$_2$, [(2-(2,4-difluorophenyl)pyridine)$_2$IrCl]$_2$, [(2-(2,4-difluorophenyl)-4-dimethylaminopyridine)$_2$IrCl]$_2$, and [(2-(3,5-difluorophenyl)-4-dimethylaminopyridine)$_2$IrCl]$_2$. The iridium dimmers were synthesized using literature procedure by reacting $IrCl_3 \cdot 3H_2O$ and 2.5 equiv of corresponding ligand by heating at 110 °C in a mixture of 2-ethoxyethanol and water (3:1, v/v) overnight under nitrogen. In a typical reaction, the [(2-phenyl-4-dimethylaminopyridine)$_2$IrCl]$_2$ dimer was synthesized using the following procedure.

[(2-Phenyl-4-dimethylaminopyridine)$_2$IrCl]$_2$. $IrCl_3 \cdot 3H_2O$ and 2.5 equiv of 2-phenyl-4-dimethylaminopyridine were heated at 110 °C in a mixture of 2-ethoxyethanol and water (3:1, v/v) overnight under nitrogen. After being cooled to room temperature, the resulting precipitate was filtered off, successively washed with methanol then Et_2O and finally dried to afford the desired dimer.

Complexes **1**−**5** were synthesized using the literature procedure.[4] In a typical reaction, the dimeric iridium (III) complex [(2-phenyl-4-dimethylaminopyridine)$_2$IrCl]$_2$ (200 mg) was dissolved in 30 mL of dichloromethane solvent under nitrogen. To this solution was added tetrabutylammonium cyanide (430 mg) ligand. The reaction mixture was refluxed with stirring for 5 h. Then, to the solution was added 1:1 solvent mixture of diethyl ether and low-boiling petroleum ether (60 mL). The precipitated solid was collected and recrystallized from methanol and low-boiling petroleum ether. The air-dried product was 230 mg, yield 81%.

1. ^{1}H NMR 200 MHz, (DMSO-d_6, δ): 0.93 (12H, t, CH_3); 1.29 (8H, q, CH_2); 1.48 (8H, m, CH_2); 3.15 (8H, t, CH_2); 6.08 (2H, d, J = 7.2); 6.60 (2H, t, J = 7.1); 6.73 (2H, t, J = 7.2); 7.3 (2H, t, J = 7.2); 7.65 (2H, d, 7.4); 7.89 (2H, t, J = 7.3); 8.07(2H, d, J = 7.8); 9.53 (2H, d, J = 5.9). The mass spectrum of [Ir(2-phenylpyridine)$_2$(CN)$_2$]$^-$ shows a peak at m/z 553.1.

2. ^{1}H NMR 200 MHz, (DMSO-d_6, δ): 0.93 (12H, t, CH_3); 1.28 (8H, q, CH_2); 1.55 (8H, m, CH_2); 3.15 (8H, t, CH_2); 3.19 (s, 12 H); 6.21 (2H, dd, J = 7.2, 1.0); 6.60 (6H, m); 7.11 (2H, d, J = 2.5); 7.57 (2H, d, 7.14); 8.95 (2H, d, J = 6.44). The mass spectrum of [Ir(2-phenyl)-4-dimethylaminopyridine)$_2$(CN)$_2$]$^-$ shows a peak at m/z 639.18.

3. ^{1}H NMR 200 MHz, (CD_2Cl_2, δ): 0.94 (12H, t, CH_3); 1.31 (8H, q, CH_2); 1.55 (8H, m, CH_2); 3.15 (8H, t, CH_2); 5.75 (2H, dd, J = 8.2, 2.1); 6.23 (2H, dt, J = 8, 2.0); 6.35 (2H, dd, J = 8.2, 2.0); 7.45 (2H, t, 7.2); 8.45 (2H, t, 7.2); 8.97 (2H, d, J = 7.3). The mass spectrum of [Ir(2-(2,4-difluorophenyl)-pyridine)$_2$(CN)$_2$]$^-$ shows a peak at m/z 625.16.

4. ^{1}H NMR 200 MHz, (CD_2Cl_2, δ): 0.94 (12H, t, CH_3); 1.31 (8H, q, CH_2); 1.55 (8H, m, CH_2); 3.15 (8H, t, CH_2); 3.21 (s, 12 H); 5.65 (2H, dd, J = 8.3, 2.4); 6.26 (2H, dt, J = 8, 2.0); 6.39 (2H, dd, J = 8.2, 2.0); 7.45 (2H, t, 3.2); 9.07 (2H, d, J = 6.89). The mass spectrum of [Ir(2,4-difluorophenyl)-4-dimethylaminopyridine)$_2$(CN)$_2$]$^-$ shows a peak at m/z 711.15.

5. ^{1}H NMR 200 MHz, (CD_2Cl_2, δ): 0.92 (12H, t, CH_3); 1.27 (8H, q, CH_2); 1.51 (8H, m, CH_2); 3.14 (8H, t, CH_2); 3.17 (s, 12 H); 6.24 (2H, dt, J = 8, 2.0); 6.53 (2H, dd J = 6.95, 2.6); 7.10 (2H, d, J = 2.5); 7.50 (2H, dd, 10.64, 2.1);8.98 (2H, d, J = 6.92). The mass spectrum of [Ir(2-(3,5-difluorophenyl)-4-dimethylaminopyridine)$_2$(CN)$_2$]$^-$ shows a peak at m/z 711.15.

Computational Details. The geometries of the investigated **1**−**5** complexes were optimized under C_2 symmetry constraints using the BP86 exchange−correlation function,[39,40] together with a TZP (DZP) basis set for Ir (N, C, H), including scalar-relativistic corrections as implemented in the ADF program.[41] On the optimized geometries we performed single-point calculations at the B3LYP/LANL2DZ[42,43] level of theory in dichloromethane solution by means of the PCM solvation model,[44,45] as implemented in the Gaussian 03 program package.[46] The lowest 10 singlet−singlet and singlet−triplet excitations have been computed by means of TDDFT for complexes **1**−**5** at both the ground state singlet S_0 and lowest excited triplet state T_1 optimized geometries. Characterization of the nature of the TDDFT transitions in terms of single orbital excitations is usually possible, provided one has access to the eigenvectors. The latter are made up of two component vectors, X and Y, related to single-particle excitations and de-excitations, respectively. In Gaussian 03, however, the program only provides the (dominant) components of the sum vector $X + Y$, and it is thus impossible in principle to separate the interfering excitation and de-excitation components. To the extent, however, that we may reasonably assume that the de-excitation vector Y is small compared to X (it would exactly be zero in the Tamm−Dancoff or single excitation CI approximation), we may take the square of the $X + Y$ vector components as a qualitative measure of the weight pertaining to the corresponding single excitations.

Acknowledgment. We acknowledge financial support of this work by the European Union (HETEROMOLMAT) and

(39) Becke, A. D. *Phys. Rev. A* **1988**, *38*, 3098.
(40) Perdew, J. P. *Phys. Rev. B* **1986**, *33*, 8822.
(41) te Velde, G.; Bickelhaupt, M. F.; Baerends, E. J.; Fonseca-Guerra, C.; van Gisbergen, S. J. A.; Snijders, J. G.; Ziegler, T. J. *Comp. Chem.* **2001**, *22*, 931.
(42) Becke, A. D. *J. Chem. Phys.* **1993**, *98*, 5648.
(43) Hay, P. J.; Wadt, W. R. *J. Chem. Phys.* **1985**, *82*, 270.
(44) Miertus, S.; Scrocco, S.; Tomasi, T. *Chem. Phys.* **1981**, *55*, 117.
(45) Cossi, M.; Barone, V. J. *Chem. Phys.* **2001**, *115*, 4708.
(46) Frisch, M. J.; Trucks, G. W.; Schlegel, H. B.; Scuseria, G. E.; Robb, M. A.; Cheeseman, J. R.; Montgomery, J. A., Jr.; Vreven, T.; Kudin, K. N.; Burant, J. C.; Millam, J. M.; Iyengar, S. S.; Tomasi, J.; Barone, V.; Mennucci, B.; Cossi, M.; Scalmani, G.; Rega, N.; Petersson, G. A.; Nakatsuji, H.; Hada, M.; Ehara, M.; Toyota, K.; Fukuda, R.; Hasegawa, J.; Ishida, M.; Nakajima, T.; Honda, Y.; Kitao, O.; Nakai, H.; Klene, M.; Li, X.; Knox, J. E.; Hratchian, H. P.; Cross, J. B.; Bakken, V.; Adamo, C.; Jaramillo, J.; Gomperts, R.; Stratmann, R. E.; Yazyev, O.; Austin, A. J.; Cammi, R.; Pomelli, C.; Ochterski, J. W.; Ayala, P. Y.; Morokuma, K.; Voth, G. A.; Salvador, P.; Dannenberg, J. J.; Zakrzewski, V. G.; Dapprich, S.; Daniels, A. D.; Strain, M. C.; Farkas, O.; Malick, D. K.; Rabuck, A. D.; Raghavachari, K.; Foresman, J. B.; Ortiz, J. V.; Cui, Q.; Baboul, A. G.; Clifford, S.; Cioslowski, J.; Stefanov, B. B.; Liu, G.; Liashenko, A.; Piskorz, P.; Komaromi, I.; Martin, R. L.; Fox, D. J.; Keith, T.; Al-Laham, M. A.; Peng, C. Y.; Nanayakkara, A.; Challacombe, M.; Gill, P. M. W.; Johnson, B.; Chen, W.; Wong, M. W.; Gonzalez, C.; Pople, J. A. *Gaussian 03*, revision C.02; Gaussian, Inc.: Wallingford, CT, 2004.

Philips Research Laboratories. S.F. and F.D.A thank MIUR (FIRB 2003: Molecular compounds and hybrid nanostructured materials with resonant and non resonant optical properties for photonic devices) and CNR (PROMO 2006) for financial support. We thank Dr. Rosario Scopelliti and Dr. Alain Razaname for X-ray and mass spectrometry service, respectively.

Supporting Information Available: Additional data. This material is available free of charge via the Internet at http://pubs.acs.org.

IC701814H